

On a class of nonlocal nonlinear Schrödinger equations and wave collapse

M. Ablowitz¹, I. Bakirtas^{2,a}, and B. Ilan³

¹ Department of Applied Mathematics, University of Colorado, Colorado 80309-0526, USA

² ITU Department of Mathematics, Istanbul Technical University, Maslak 34469, Istanbul, Turkey

³ School of Natural Sciences UC Merced, PO Box 2039, Merced, CA 95344, USA

Abstract. A similar type of nonlocal nonlinear Schrödinger (NLS) system arises in both water waves and nonlinear optics. The nonlocality is due to a coupling between the first harmonic and a mean term. These systems are termed nonlinear Schrödinger with mean or NLSM systems. They were first derived in water waves by Benney-Roskes and later by Davey-Stewartson. Subsequently similar equations were derived and found to be fundamental systems in quadratically nonlinear optical media. Wave collapse can occur in these systems. The collapse structure and the role of the ground state in the collapse process are studied. There are similarities to the well-known collapse mechanism associated with classical NLS system. Numerical simulations show that NLSM collapse occurs with a quasi-self-similar profile that is a modulation of the corresponding ground-state. Further, it is found that NLSM collapse can be arrested by adding small nonlinear saturation.

1 Introduction

Nonlinear wave phenomena have wide physical and mathematical interest. They arise broadly in fields such as nonlinear optics, fluid dynamics, lattice dynamics, plasma physics, and elasticity (cf. [1–3]). The solutions of the governing nonlinear waves equations exhibit important phenomena, such as stable localized waves or solitons, self-similar structures, chaotic dynamics and wave singularities such as shock waves which have discontinuities in the derivatives and/or wave collapse, i.e., blowup, where the solution tends to infinity in finite time or finite propagation distance. A paradigm equation that arises naturally in *cubic media*, such as Kerr media in optics, is the (2+1)D focusing cubic nonlinear Schrödinger equation (NLS),

$$iu_z(x, y, z) + \frac{1}{2}\Delta u + |u|^2u = 0, \quad u(x, y, 0) = u_0(x, y), \quad (1)$$

where u is the slowly-varying envelope of the optical wave, z is the direction of propagation, (x, y) are the transverse directions, $\Delta u \equiv u_{xx} + u_{yy}$, and u_0 represents the initial conditions. Remarkably, in 1965 Kelley [4] carried out direct numerical calculations of (1) that indicated the possibility of wave collapse. In 1970 Vlasov et al. [5] proved that solutions of equation (1) satisfy the so-called “Virial Theorem” (also called Variance Identity), i.e.,

$$\frac{d^2}{dz^2}V(z) \equiv \frac{d^2}{dz^2} \int (x^2 + y^2)|u|^2 = 4H, \quad H = \frac{1}{2} \int (|\nabla u_0|^2 - |u_0|^4), \quad (2)$$

where $\nabla \equiv (\partial_x, \partial_y)$, the integrations are carried over the (x, y) plane, and H is the Hamiltonian of equation (1), which is also a constant of motion. Using this Theorem, Vlasov et al. concluded

^a e-mail: ilkayb@itu.edu.tr

that the solution of the NLS can become singular in finite distance (or time), because a positive-definite quantity could become negative for initial conditions satisfying $H < 0$. Subsequently, Weinstein [6] showed that when the power (which is also conserved) is sufficiently small, i.e., $N = \int |u_0|^2 = \text{const} < N_c$, the solution exists globally, i.e., for all $z > 0$.

Therefore, a *sufficient condition* for collapse is $H < 0$ while a *necessary condition* for collapse is $N > N_c$. Weinstein also found that the *ground-state* of the NLS plays an important role in the collapse theory. The ground-state is a stationary solution of the form $u = R(r)e^{it}$, such that R is radially-symmetric, positive, and monotonically decaying. The ground state is also obtained from a variational principle (cf. [6]). Papanicolaou et al. [7] studied the singularity structure near the collapse point and showed asymptotically and numerically that collapse occurs with a quasi self-similar profile. The readers are referred to [8] for comprehensive reviews of this issue and related studies of NLS systems. Recently, Merle and Raphael [9] analyzed in detail the collapse behavior of NLS equation (1) and related equations and rigorously elucidated the role of the self-similar asymptotic profile as collapse occurs. Interestingly, Gaeta et al. [10] have recently carried out optical experiments in cubic media that reveal the nature of the singularity formation. They find experimentally that collapse occurs with a self-similar profile.

There are considerably fewer studies of wave collapse, whose governing system of equations have *quadratic nonlinearities*, two cases being water waves and χ^2 nonlinear-optical media. Here we discuss a class of related systems of which special cases are sometimes referred to as Benney-Roskes [11] or Davey-Stewartson [12] type. More generally we refer to these systems as NLS with mean or **NLSM**. The physical derivation of NLSM systems in water waves and nonlinear optics is reviewed in section 2. Broadly speaking, the derivation of NLSM systems is based on an expansion of the slowly-varying (i.e., quasi-monochromatic) wave amplitude in the first and second harmonics of the fundamental frequency, as well as a mean term that corresponds to the zero'th harmonic. This leads to a system of equations that describes the nonlocal-nonlinear coupling between a dynamic field that is associated with the first harmonic (with a ‘‘cascaded’’ effect from the second harmonic), and a static field that is associated with the mean term. For the physical interesting models considered here, the general NLSM system can be written in the following non-dimensional form,

$$iu_z + \frac{1}{2}(\sigma_1 u_{xx} + u_{yy}) + \sigma_2 u |u|^2 - \rho u \phi_x = 0, \quad \phi_{xx} + \nu \phi_{yy} = (|u|^2)_x, \quad (3)$$

where $u(x, y, t)$ corresponds to the field associated with the first-harmonic, $\phi(x, y, t)$ corresponds to the mean field, σ_1 and σ_2 are ± 1 , and ν and ρ are real constants that depend on the physical parameters. It is known that System (1) can admit wave collapse when $\sigma_1 = \sigma_2 = 1$ and $\nu > 0$. In that case, the governing equations are

$$iu_z + \frac{1}{2}\Delta u + |u|^2 u - \rho u \phi_x = 0, \quad (4a)$$

$$\phi_{xx} + \nu \phi_{yy} = (|u|^2)_x, \quad (4b)$$

where $\nu > 0$ and ρ is real, and the initial conditions are $u(x, y, 0) = u_0(x, y)$, $\phi(x, y, 0) = \phi_0(x, y)$, such that equation (4b) is satisfied at $z = 0$, i.e., $\phi_{0,xx} + \nu \phi_{0,yy} = (|u_0|^2)_x$. The goal of this study is to further investigate the collapse dynamics in the NLSM System (4).

Note that System (4) reduces to the classical NLS equation (1) when $\rho = 0$. In this case the mean field ϕ does not couple to the harmonic field u in equation (4a). In addition, when $\nu = 0$ equation (4b) gives that $\phi_x = |u|^2$ and, therefore, equation (4a) reduces to a classical NLS equation (1) with the cubic term $(1 - \rho)|u|^2 u$. In optics we have: $\rho > 0$, whereas in water waves it turns out that $\rho < 0$. We find that the collapse mechanism is ‘‘stronger’’ when $\rho < 0$. Strictly speaking, whenever $\rho \neq 0$ and $\nu \neq 0$ the NLSM System (4) is a nonlocal system of equations. Indeed, since $\nu > 0$, equation (4b) can be solved as

$$\phi(x, y, z) = \int_{-\infty}^{\infty} G(x - x', y - y') \frac{\partial}{\partial x'} |u(x', y', z)|^2 dx' dy',$$

where $G(x, y)$ is the usual Green's function. For equation (4b) $G(x, y) = (4\pi)^{-1} \log(x^2 + y^2/\nu)$, which corresponds to a strongly-nonlocal function ϕ . Although some research has indicated

that some types of strong nonlocality can arrest collapse, we do not find this to be the case for System (4). Indeed there is a striking mathematical similarity between collapse dynamics in the NLS and NLSM cases.

An outline of the paper is as follows:

1. In section 2 the physical interesting NLSM systems that arise in water waves and in nonlinear optics are discussed.
2. In section 3 the theory of global existence in NLS and NLSM equations and wave collapse is reviewed. It is shown, via the Hamiltonian why collapse in the case of water waves ($\rho < 0$) is relatively easier to attain, and also occurs more quickly, than in the case of nonlinear optics ($\rho > 0$).
3. Employing numerical calculations of the ground-state and global existence theory, in Section 4 the necessary criteria for collapse is studied in terms of the parameters ν and ρ in the NLSM System (4). Using the Virial Theorem and the Hamiltonian, a sufficient condition for collapse is found and employed for Gaussian input beams, explicitly in terms of ν , ρ , and the input power. These theoretical results are shown to be consistent with numerical simulations of the NLSM System (4). They are also consistent with the numerical results of Crasovan et al. [13] who studied the nonlinear optics ($\rho > 0$) case. The effect of input astigmatism in the initial conditions on the critical power for collapse is also analyzed (section 4.1)). In section 4.2 it is shown that the NLSM can admit collapse even without the cubic term [i.e., without $|u|^2u$ in equation (4a)].
4. In section 5 the astigmatism of the NLSM ground-state is considered in the (ν, ρ) parameter space. The ground-state is found to be relatively more astigmatic in nonlinear optics ($\rho > 0$) than in water-waves ($\rho < 0$). The dependence of the astigmatism of the ground-state on ν is seen to be relatively weaker than its dependence on ρ .
5. In section 6 the nature of NLSM wave collapse is investigated using direct numerical simulations of the NLSM System (4). The simulations indicate that the solution near the collapse point is well described by a quasi self-similar profile that is given in terms of a modulation of the ground state. The self-similar collapse is further explored by comparing the NLSM solution to the ground-state itself. The ground-state is calculated by employing an effective fixed-point algorithm which has been successfully previously applied in many cases; e.g. dispersion-managed NLS theory. The numerical results show that the ground-state plays a central role in the collapse process. This strengthens the results of Papanicolaou et al. [14] associated with the NLSM system and is also in the same spirit as the corresponding results for the classical NLS equation.
6. In section 7 it is shown using numerical simulations that NLSM collapse can be arrested by adding small saturation to the nonlinearity. This is a phenomenon that can be explained by employing the results of Fibich and Papanicolaou [15] for the the perturbed NLS.

2 Applications of NLSM systems to water-waves and nonlinear optics

In this section we outline the main results associated with the derivations of NLSM systems for water waves and nonlinear optics. The derivations follow from weakly-nonlinear quasi-monochromatic asymptotic expansions. In the case of water waves some early results regarding collapse were obtained and these are also mentioned in this section.

2.1 Water waves

The asymptotic expansion of the velocity potential ϕ and wave height η in the case of free-surface gravity-capillary water waves, takes the form

$$\phi \sim \varepsilon[\tilde{A}e^{i(kx-wt)} + \text{c.c.} + \tilde{\Phi}] + \varepsilon^2[\tilde{A}_2e^{2i(kx-wt)} + \text{c.c.}] + \dots, \quad (5a)$$

$$\eta \sim \varepsilon[\tilde{B}e^{i(kx-wt)} + \text{c.c.}] + \varepsilon^2[\tilde{B}_2e^{2i(kx-wt)} + \text{c.c.} + \tilde{\eta}] + \dots, \quad (5b)$$

where $\varepsilon \ll 1$ is a measure of the (weak) nonlinearity, \tilde{A} , \tilde{B} , \tilde{A}_2 , \tilde{B}_2 , and $\tilde{\Phi}$, $\tilde{\eta}$ are slowly varying functions of (x, y, t) , corresponding to the coefficients of the first, second, and zero'th harmonics, respectively, "c.c." denotes complex conjugate of the term to its left, and the frequency ω satisfies the dispersion relation $\omega^2(\kappa) = (g\kappa + T\kappa^3) \tanh(\kappa h)$, where g is the gravity acceleration, T is the surface tension coefficient, and $\kappa = \sqrt{k^2 + l^2}$, where (k, l) are the wave-numbers in the (x, y) directions, respectively. Substituting the expansions (5) into the water-waves equations (i.e., Euler's equation with a free surface) and assuming slow modulations of the field in the x and y directions yields a nonlinearly-coupled system for \tilde{A} and $\tilde{\Phi}$. After non-dimensionalization, i.e., $(A, \Phi) = (\tilde{A}, \tilde{\Phi})k^2/\sqrt{gh}$, one finds the general NLSM system (cf. [16] and references therein)

$$iA_\tau + \lambda A_{\xi\xi} + \mu A_{\eta\eta} = \chi|A|^2 A + \chi_1 A \Phi_\xi, \quad (6a)$$

$$\alpha \Phi_{\xi\xi} + \Phi_{\eta\eta} = -\beta(|A|^2)_\xi, \quad (6b)$$

where $\xi = \varepsilon k(x - c_g t)$, $\eta = \varepsilon l y$ and $\tau = \varepsilon^2 \sqrt{gk} t$ are dimensionless coordinates, and $c_g = \partial\omega/\partial k$ is group velocity. The coefficients $\lambda, \mu \geq 0$, $\chi, \chi_1 \geq 0$, α and $\beta \geq 0$ are functions of h, T, k, c_g , and the second-order dispersion coefficients $\partial^2\omega/\partial k^2$ and $\partial^2\omega/\partial l^2$. We note that in the derivation of System (6) all coefficients in the wave height, η , expansion may be obtained in terms of the coefficients in the velocity potential, ϕ , expansion. Similarly the term \tilde{A}_2 is expressed in terms of \tilde{A} , which accounts for the fact that A_2 does not appear explicitly in the resulting system¹. Also it should be noted that the mean term in the wave height is at $O(\varepsilon^2)$ whereas the mean term in the velocity potential is at $O(\varepsilon)$. The discrepancy is due to the fact that the velocity potential itself is not a "physical" variable. However, the velocity is obtained as a derivative of the potential, $\mathbf{u} = \nabla\phi$, in which case the mean term for the velocity drops down one order to $O(\varepsilon^2)$ because $\tilde{\Phi}$ is slowly-varying. This is consistent with the expansion for the physical variable η representing the wave height.

NLSM equations were originally obtained by Benney and Roskes [11] in their study of the instability of wave packets in water of finite depth h , without surface tension. In 1974, Davey and Stewartson [12] analyzed the evolution of a 3D wave packet in water of finite depth and obtained a different, although equivalent, form of these equations. Their form is more similar to the equations given above. In 1975 Ablowitz and Haberman [17] studied the integrability of systems such as (6). These integrable systems correspond to the Benney-Roskes equations in the shallow water limit. In 1977 Djordevic and Reddekopp [18] extended the results of Benney and Roskes to include surface tension. Subsequently, Ablowitz and Segur [16] investigated System (6) or, equivalently, System (3). They showed that the shallow water limit, i.e., $h \rightarrow 0$, corresponds to $\sigma_1 \rightarrow -\nu = \pm 1$, and $\rho \rightarrow 2$ in system (3). The resulting equations agreed with those obtained by Ablowitz and Haberman [17]. Thus, the shallow-water limit of System (6) could be obtained from an associated compatible linear scattering system. In [19] these reduced equations were linearized by the inverse scattering transform (see also [20]). Thus the shallow-water limit of equation (6) is integrable.

Ablowitz and Segur [16] also studied the NLSM System (6) in the non-integrable case. In this parameter regime, System (6) can be transformed by a rescaling of variables to System (3) with $\sigma_1 = \sigma_2 = 1$ and $\nu > 0$, i.e., the so called focusing elliptic-elliptic case, which, physically speaking, requires sufficiently large surface tension. They found that System (6) preserves the Hamiltonian

$$H = \int \left[\lambda \left| \frac{\partial A}{\partial \xi} \right|^2 + \mu \left| \frac{\partial A}{\partial \eta} \right|^2 \right] - \frac{1}{2} \int \left[(-\chi)|A|^4 + \frac{\alpha\chi_1}{\beta}(\Phi_\xi)^2 + \frac{\chi_1}{\beta}(\Phi_\eta)^2 \right], \quad (7)$$

where the first and second integrals correspond to the second-derivative and the nonlinear terms in equation (6a), respectively, and the integrations are carried over the (ξ, η) plane. When, in addition to the physical requirements $\mu \geq 0$, $\beta \geq 0$, and $\chi_1 \geq 0$, one has that $\lambda > 0$, $-\chi > 0$, and $\alpha > 0$, the first and second integral terms in (7) are positive and negative-definite, respectively. This corresponds to the self-focusing regime. Clearly, in that case $H < 0$ is possible

¹ A similar observation holds in the optics case mentioned below.

for sufficiently large initial conditions; i.e. $|A|$ sufficiently large². Furthermore they proved that the following Virial Theorem holds

$$\frac{\partial^2}{\partial \tau^2} \int \left(\frac{\xi^2}{\lambda} + \frac{\eta^2}{\mu} \right) |A|^2 = 8H .$$

It can be seen, if $H < 0$, the moment of inertia vanishes at a finite time. In that case, as for the NLS case mentioned above, this indicates finite-distance singularity formation. We note that in this study collapse solutions with the self-similar profile $|A| \sim L^{-1}(t)f(x/L(t), y/L(t))$ were also investigated.

2.2 Nonlinear optics

It is well-known that the electric polarization field of intense laser beams propagating in optical media can be expanded in powers of the electric field as

$$P = \chi^{(1)} * E + \chi^{(2)} * E * E + \chi^{(3)} * E * E * E + \dots , \tag{8}$$

where $E = (E_1, E_2, E_3)$ the the electric field vector and $\chi^{(j)}$ are the susceptibility tensor coefficients of the medium. In isotropic Kerr media, where the nonlinear response of the material depends cubically [i.e., through $\chi^{(3)}$ and when $\chi^{(2)} \equiv 0$] and instantaneously on the applied field, the dynamics of quasi-monochromatic optical pulses is governed by the NLS equation (1) (cf. [4, 21, 22]). Importantly, it turns out that NLSM type equations arise in nonlinear optics when studying media with a non-zero $\chi^{(2)}$, i.e., materials that have a *quadratic* nonlinear response. Such materials are anisotropic, e.g., crystals whose optical refraction has a preferred direction.

Ablowitz, Biondini and Blair [23, 24] showed, from first principles, that NLSM type equations describe the evolution of the electromagnetic field in such quadratically [i.e., $\chi^{(2)}$] polarized media. Both scalar and vector (3+1)D NLS systems were obtained. Vector NLSM systems have no analog in water waves. In the derivation, of say the scalar problem, a quasi-monochromatic expansion of the electromagnetic field is assumed. The first terms with the fundamental harmonic, second-harmonic, and a mean term take the form

$$E_1 \sim \varepsilon [A e^{i(kx - \omega t)} + c.c.] + \varepsilon^2 [A_2 e^{2i(kx - \omega t)} + c.c. + \phi_x] + \dots , \tag{9}$$

where A , A_2 , and ϕ are slowly varying functions of (x, y, t) , which correspond to the first, second, and zero'th harmonics, respectively. Using the polarization structure above (8), substituting the expansions into Maxwell's equations leads to the following system of equations

$$[2ik\partial_Z + (1 - \alpha_{x,1})\partial_{XX} + \partial_{YY} - kk''\partial_{TT} + M_{x,1}|A|^2 + M_{x,0}\phi_x]A = 0, \tag{10a}$$

$$[(1 - \alpha_{x,0})\partial_{XX} + \partial_{YY} + s_x\partial_{TT}]\phi_x - \alpha_{y,0}\partial_{XY}\phi_y = (N_{x,1}\partial_{TT} - N_{x,2}\partial_{XX})|A|^2, \tag{10b}$$

where $\alpha_{x,0}$, $\alpha_{x,1}$, $\alpha_{y,0}$, and s_x depend on the linear polarization term $\chi^{(1)}$; $M_{x,0}$, $N_{x,1}$, and $N_{x,2}$ depend on the nonlinear polarization terms $\chi^{(2)}$ and $\chi^{(3)}$; and $M_{x,1}$ depends on products of $\chi^{(2)}$ and $\chi^{(3)}$. From a physical point of view, the dependence of $M_{x,1}$ on $\chi^{(2)}$ and $\chi^{(3)}$ corresponds to the fact that the second-harmonic (i.e., \tilde{A}_2) is coupled to the first harmonic (i.e., \tilde{A}_1) via a process that is sometimes referred to as “optical rectification” or a “cascaded” optical effect. Like the water-waves case, in optics \tilde{A}_2 is expressed in terms of \tilde{A}_1 , which explains why A_2 does not appear explicitly in the resulting System (10). In addition, similar to the water-waves case, the term with $M_{x,0}$ in System (10a) couples the mean field to the first-harmonic field. It is important to note that, when the time dependence in these equations is neglected ($\partial_T \equiv 0$) and

² Note that from equation (6b) Φ scales as $|A|^2$, so all the terms in the second integral of (7) scale like $|A|^4$.

for media with a special symmetry class such that $\alpha_{y,0} = 0$, it can be seen that, after proper rescaling, the governing system of equation is given by System (4). In [25] these equations were further elucidated and the coefficients described in terms of the electro-optic effect.

From the point of view of perturbation analysis, we remark that in the expansion of the field in the case of water-waves [i.e., equations (5)], the mean term for the velocity potential $\bar{\Phi}$ appears as an $O(\varepsilon)$ term, whereas in the in the case of optics [i.e., equation (9)], the mean term ϕ_x appears as an $O(\varepsilon^2)$ term. But, the physically measurable quantity in water waves is $\tilde{\nabla}\bar{\Phi}$, which scales like $O(\varepsilon^2)$, because $\bar{\Phi}$ is slowly-varying. Therefore, the expansions in the water waves and optics cases are analogous from the viewpoint of perturbation analysis.

Wave collapse in such NLSM systems was investigated numerically by Crasovan et al. [13]. They solved the following normalized system of equations,

$$iU_z + \frac{1}{2}\Delta U + |U|^2U - \rho UV = 0, \quad (11a)$$

$$V_{xx} + \nu V_{yy} = (|U|^2)_{xx}, \quad (11b)$$

where U is the normalized amplitude of the envelope of the electric field, V is the normalized static field, ρ is a coupling constant that comes from the combined optical rectification and electro-optic effects, and ν corresponds to the anisotropy coefficient of the medium. They solved System (11) numerically with Gaussian initial conditions for U . The regions of collapse were studied for various values of the parameters ρ and ν . It should be noted that System (11) is a simple mathematical modification of the NLSM System (4). Indeed, starting with the NLSM System (4), taking the derivative of equation (4b) with respect to x , and defining the new variable (potential) $V = \phi_x$, one finds that the resulting system is identical to (11).

3 Wave collapse, ground-states and global existence

We first state some well-known results for the NLS and NLSM equations. Two conserved quantities for the NLS equation (1) and NLSM System (4) are the power,

$$N(u) = \int |u|^2 = N(u_0),$$

and the Hamiltonian, i.e.,

$$H_{\text{NLS}}(u) = \frac{1}{2} \int |\nabla u|^2 - \frac{1}{2} \int |u|^4 = H_{\text{NLS}}(u_0), \quad (12)$$

$$H_{\text{NLSM}}(u, \phi) = \frac{1}{2} \int |\nabla u|^2 - \frac{1}{2} \int |u|^4 + \frac{\rho}{2} \int (\phi_x^2 + \nu \phi_y^2) = H_{\text{NLSM}}(u_0, \phi_0),$$

where H_{NLS} and H_{NLSM} correspond to equation (1) and System (4), respectively, ϕ in (13) is obtained from equation (4b) and all integrations (here and below) are carried over the (x, y) plane. It can be shown that the so called Virial Theorem holds (cf. [16]),

$$\frac{\partial^2}{\partial z^2} \int (x^2 + y^2) |u|^2 = 4H. \quad (13)$$

We are interested in the localized-decaying case, when u and ϕ vanish sufficiently rapidly at infinity and are in the Sobolev space H_1 , i.e., $\int |f|^2 + \int |\nabla f|^2 < \infty$ ($f = u, \phi$). It should be noted that in the context of the water wave problem (i.e., $\rho < 0$), existence and well-posedness of solutions of System (4) were studied in [26].

It is also known in NLS and NLSM theories that when a singularity occurs, it corresponds to blowup of the gradient as well as the peak amplitude of the wave. Mathematically, this means that

$$\lim_{z \rightarrow Z_c} \int |\nabla u|^2 = \infty, \quad \lim_{z \rightarrow Z_c} \max_{(x, y)} |u(x, y, z)| = \infty,$$

where Z_c is the collapse distance. Thus, when $H < 0$ it follows from the Virial Theorem (13) that the solution becomes singular in finite time. This gives a *sufficient condition* for collapse. A *necessary condition* for collapse can also be obtained using the associated ground-state; this is discussed below. Note that the Hamiltonian (13) is comprised of three integrals, the first of which is positive definite, the second negative definite, and the third integral is also definite with a sign that is determined by ρ . NLS (and NLSM) theory indicates that the positive-definite terms correspond to a defocusing mechanism, while the negative-definite terms correspond to a focusing mechanism. It follows that when $\rho > 0$, i.e., in the optics case, the coupling to the mean field corresponds to a self-defocusing mechanism, while when $\rho < 0$, i.e., the water-waves case, it corresponds to a self-focusing effect in addition to the the cubic term in the NLS equation (1). In this framework, one expects that self-focusing in the water-waves case is “easier” to attain than in the optics case. We confirm this in numerical simulations (see sections 4 and 6 for details).

A stationary solution of the NLSM System (4) has a solution of the form $u(x, y, z) = F(x, y)e^{i\lambda z}$ and $\phi(x, y, z) = G(x, y)$, where F and G are real functions and λ is a positive real number. Substituting this ansatz into System (4) leads to the following coupled system

$$-\lambda F + \frac{1}{2}\Delta F + F^3 - \rho F G_x = 0, \tag{14a}$$

$$G_{xx} + \nu G_{yy} = (F^2)_x. \tag{14b}$$

On the other hand, the NLS stationary solutions, which are obtained by substituting $u = R(x, y)e^{i\lambda z}$ into the NLS equation (1), satisfy

$$-\lambda R + \frac{1}{2}\Delta R + R^3 = 0. \tag{15}$$

The *ground-state* of the NLS³ can be defined as a solution in H_1 of equation (15) for a given λ having minimal power of all the nontrivial solutions. Existence and uniqueness of the ground state has been proven, as also the fact that it is radially-symmetric, positive, and monotonically decaying (see [8]). Since $R(r; \lambda) = \sqrt{\lambda}R(\sqrt{\lambda}r; 1)$, it suffices to consider the case $\lambda = 1$. This solution will be denoted by R . Furthermore, Weinstein [6] proved that the NLS ground-state is a minimizer of a Gagliardo-Nirenberg inequality that is associated with the NLS Hamiltonian. To be precise, the functional

$$J(u) = \frac{\|u\|_2^2 \|\nabla u\|_2^2}{\|u\|_4^4}, \quad \|u\|_p^p \equiv \int |u|^p,$$

attains its minimum for $u \in H_1$ when $u(x, y) = R(r)$, where R is the ground-state of equation (15) and $J(R) = 2/N_c$, where $N_c \equiv \int R^2$. Moreover, Weinstein proved that when $N < N_c$, the NLS solution exists globally, i.e. for all $z > 0$, in H_1 . In addition, it is not difficult to show that any stationary solution, in particular the ground-state, admits a zero Hamiltonian, i.e., $H_{\text{NLS}}(R) = 0$. These results explain why the ground-state may be considered to be on the borderline between existence and collapse. Indeed, if one considers the initial conditions $u_0 = (1 + \varepsilon)R(r)$ with $\varepsilon = \text{const}$. When $\varepsilon < 0$ then $N < N_c$ and, therefore, the solution exists globally. On the other hand, when $\varepsilon > 0$ then $H < 0$ and, therefore, finite-distance collapse is guaranteed by the Virial Theorem (cf. [6]). We note that $N \geq N_c$ is only a necessary condition for collapse; namely there are solutions with $N > N_c$ that exist globally.

In a similar spirit to the NLS case, the ground-state of System (14) can be defined as the nontrivial solution (F, G) in H_1 , such that F has minimal power. Cipolatti [27] proved the existence of the ground-state. In the same spirit as for the NLS, Papanicolaou et al. [14] defined the ground-state as the minimizer the associated functional⁴

$$J(u) = \frac{\|u\|_2^2 \|\nabla u\|_2^2}{\int [|u|^4 + \mathcal{B}(u)u^{*2}]}, \quad \mathcal{B}(u) \equiv \mathcal{F}^{-1} \left[\frac{\rho k_x^2}{k_x^2 + \nu k_y^2} \mathcal{F}[|u|^2] \right],$$

³ R , the NLS ground-state, is sometimes referred to as the Townes profile.

⁴ Note that from equation (4b) $\phi_x = \rho^{-1}\mathcal{B}(u)$.

where \mathcal{F} and \mathcal{F}^{-1} denote the Fourier Transform operator and its inverse, respectively. They extended global existence theory to the NLSM and proved the following result:

Theorem 1 Consider System (4) with initial conditions $u_0 \in H_1$. Let F be the nontrivial minimizer of $J(u)$ above, and let N_c be defined as

$$N_c(\nu, \rho) \equiv \int F^2(x, y; \nu, \rho). \quad (16)$$

Then F is a positive function and, therefore, $N_c > 0$. In addition, if $\int |u_0|^2 < N_c$ the solution of System (4) exists in H_1 for all $z > 0$.

Thus solutions of the NLSM System (4) exist globally when their power is smaller than the power of the corresponding ground-state.

On the other hand, since the ground-state is a stationary solution, from the Virial Theorem (13), in analogy to $H_{\text{NLS}}(R) = 0$, one has also

Proposition 1 Let (F, G) be a solution of System (14). Then

$$H_{\text{NLSM}}(F, G) \equiv \frac{1}{2} \int (\nabla F)^2 - \frac{1}{2} \int F^4 + \frac{\rho}{2} \int (\nabla_\nu G)^2 = 0, \quad (17)$$

where $(\nabla_\nu G)^2 \equiv G_x^2 + \nu G_y^2$.

Therefore, it follows from Theorem 1, the Virial Theorem (13), and Proposition 1 that, as in the NLS case, the NLSM ground-state is neutrally-stable and it may be considered to be a borderline case between global existence and collapse.

4 Parameter regimes of wave collapse and global-existence

In this section System (4) is analyzed with the following Gaussian initial conditions

$$u_0^G(x, y) = \sqrt{\frac{2N}{\pi}} e^{-(x^2+y^2)}, \quad (18)$$

where $N = N(G)$ is the input power of u_0^G . Then the collapse and global-existence regions in the NLSM System (4) are explored in the (N, ν, ρ) parameter space by employing the Virial Theorem (13), the global-existence Theorem (1), and direct (2+1)D numerical simulations of the NLSM System (4).

The critical power $N_c(\nu, \rho)$ is calculated from the ground-state which is found by using a fixed-point numerical procedure similar to that recently used in dispersion-managed soliton theory (cf. [29,30]). Periodic boundary conditions are used in the fixed point procedure. For the NLSM simulations a standard 4'th order accurate Runge-Kutta integration is used, with 4'th order accurate spatial finite-differences in x, y . The computational domain truncates the (x, y) plane and employs Dirichlet boundary-conditions at $|x| = L$ and $|y| = L$, where L is taken sufficiently large, so to assure that the results are independent of reflections from the outer boundaries.

Substituting the initial-conditions (18) into the NLSM Hamiltonian (13) gives

$$H(u_0^G, \phi_0^G) = N - \left(1 - \frac{\rho}{1 + \sqrt{\nu}} \right) \frac{N^2}{2\pi}. \quad (19)$$

From (19) and the Virial Theorem (13) it follows that for the Gaussian initial conditions (18) there is a *threshold power* for which $H = 0$, given by

$$N_c^H(\nu, \rho) \equiv \frac{2\pi}{1 - \rho/(1 + \sqrt{\nu})}, \quad (20)$$

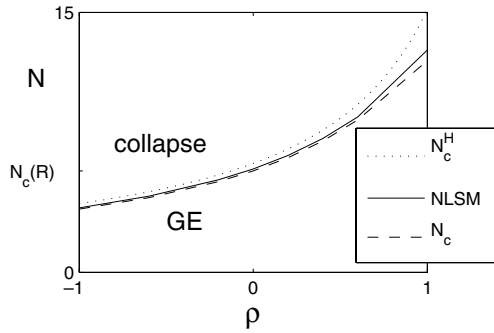


Fig. 1. The critical power to obtain collapse as a function of ρ for $\nu = 0.5$ (recall: $\rho < 0$ for water-waves and $\rho > 0$ for optics). N_c is obtained from the power of the ground-state [i.e., equation (16), dashes], N_c^H corresponds to $H = 0$ [i.e., equation (20), dotted], and the threshold power for collapse obtained by direct numerical simulation of the NLSM [i.e., System (4) with (18), solid]. “GE” denotes global existence and “NLSM” denotes direct numerical simulations of System (4).

such that when $N > N_c^H$ then $H < 0$ and, therefore, the solution collapses at finite distance. We note that this condition makes sense only when $0 < N_H < \infty$, which implies $\rho < 1 + \sqrt{\nu}$. Conversely, when either $\rho \geq 1 + \sqrt{\nu}$ (no matter how large N) or $N \leq N_c^H$, then $H \geq 0$, in which case collapse is not guaranteed by the Virial Theorem.

Figure 1 compares the critical power for collapse, N_c (16), the threshold-power N_c^H (20), and the “actual” power for collapse found from numerical simulations of the NLSM System (4), where the latter is obtained by gradually increasing the input power (or amplitude), i.e., N in the initial conditions (18), until the solution undergoes collapse. This figure also shows that for $\nu = 0.5$ and $-1 \leq \rho \leq 1$, N_c^H (20) is quite close to N_c , which, in turn, is very close to the numerically obtained threshold power for collapse in the NLSM System (4). For example, for the classical NLS (i.e., $\rho = 0$) the discrepancy between $N_c(R) \approx 1.86\pi$ and $N_c^H(R) = 2\pi$ is approximately 7% (see also [28]). In addition, in this entire parameter regime the discrepancy between N_c and the numerically-obtained threshold power is less than 2%. This figure also shows that the change in the critical power with ρ is somewhat more pronounced for $\rho > 0$ than for $\rho < 0$. In a similar manner, figure 2 shows that for a wide range of the parameters, N_c^H (20) is a good approximation of N_c , which, in turn, is a good approximation of the numerically-obtained power for collapse. Furthermore, this figure shows that the critical power is weakly-dependent on ν , for either sign of ρ .

Another way of using equation (19) is to fix N and allow ν and ρ to vary. Thus, for a fixed N there is a *separatrix curve* in the (ν, ρ) plane for which $H = 0$, given by

$$\rho_c^H(N, \nu) \equiv \left(1 - \frac{2\pi}{N} \right) (1 + \sqrt{\nu}) , \tag{21}$$

such that when $\rho < \rho_c^H$ then $H < 0$ and collapse is guaranteed by the Virial Theorem. These separatrix curves are depicted in figure 3. They are consistent in the case of $\rho > 0$ with the results of Crasovan et al. [13].

As discussed in in section 3, larger (more positive) values of ρ correspond to more defocusing. In fact, the results in this section show that when $\rho < 0$, or when $\rho > 0$ and sufficiently small,

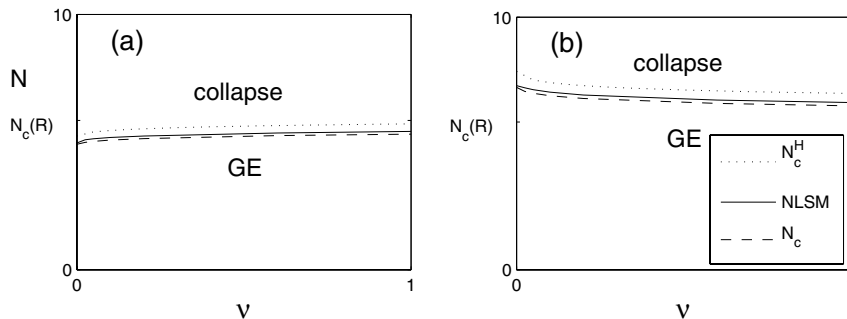


Fig. 2. Same as figure 1 with: (a) $\rho = -0.2$ and varying ν ; (b) $\rho = 0.2$ and varying ν .

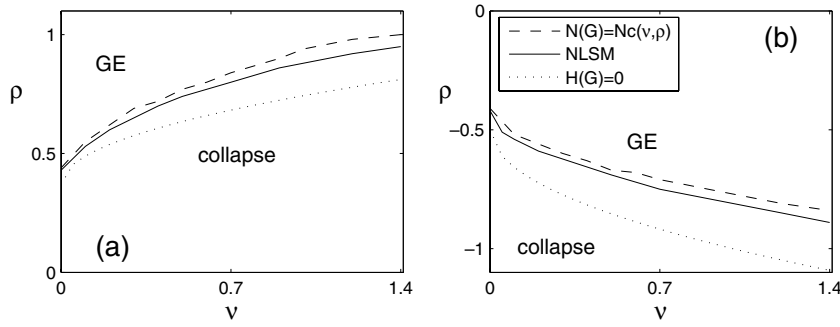


Fig. 3. The regions in the (ν, ρ) plane corresponding to collapse and global-existence (GE) are plotted. Equating the power of the ground-state, $N_c(\nu, \rho)$ [i.e., equation (16)], to the power $N(G)$ of the initial conditions (18) [dashes, denoted by $N(G) = N(\nu, \rho)$ in the legend], ρ_c^H obtained from $H = 0$ [i.e., equation (21), dotted, denoted by $H(G) = 0$ in the legend], and using direct numerical simulations of the NLSM [i.e., System (4), solid] for: (a) nonlinear optics (i.e., $\rho > 0$) and the initial conditions (18) with the fixed input power $N(G) = 10$; (b) water waves (i.e., $\rho < 0$) and the initial conditions (18) with $N(G) = 4\pi/3$.

the defocusing effect induced by the coupling to the mean field is weaker than the focusing effect induced by the cubic term in equation (4a). In that case, collapse is guaranteed by the Virial Theorem for sufficiently large input power. On the other hand, when $\rho > 0$ and is sufficiently large, the defocusing effect induced by the coupling to the mean field can overcome the focusing effect induced by the cubic term in equation (4a). In that case, the NLSM can effectively behave as a defocusing NLS-type equation, i.e., like equation (1) with a negative sign before the cubic term.

It should be emphasized that $H \geq 0$ does not imply GE, because $H < 0$ is merely a sufficient condition for collapse, it is not necessary. On the other hand, due to the explicit form and indicated accuracy, conditions (20) and (21) can be useful for predicting for the boundary in the (N, ν, ρ) space between the regions of collapse and GE. Nevertheless, the condition derived from GE theory appears to be more accurate in the following sense: the actual (numerical) critical power appears to be slightly closer to N_c than to N_c^H . We note that in [28] a similar conclusion was reached for the NLS equation (1) when using Gaussian and other similar types of initial conditions.

4.1 Initial data with astigmatism

The above results described above can be extended to the case when the initial conditions are astigmatic. Let us consider the astigmatic Gaussian initial conditions

$$u_0^E(x, y) = \sqrt{\frac{2EN}{\pi}} e^{-[(Ex)^2 + y^2]}, \quad (22)$$

where N is the input power and E is input ellipticity. Here $E = 1$ corresponds to radial symmetry, whereas $0 < E < 1$ and $E > 1$ correspond to relative elongation along the x and y axes, respectively.

In a manner similar to equation (19), one arrives at

$$H(u_0^E, \phi_0^E) = \frac{1 + E^2}{2} N - \left(1 - \frac{\rho}{1 + \sqrt{\nu}/E} \right) \frac{EN^2}{2\pi}. \quad (23)$$

If we call

$$N_c^H(\nu, \rho, E) \equiv \frac{(E + 1/E)\pi}{1 - \rho/(1 + \sqrt{\nu}/E)}, \quad (24)$$

it follows that when $N > N_c^H$ then $H < 0$ and, therefore, the solution collapses at finite distance. This condition makes sense only when $0 < N_H < \infty$, which, in turn, implies that $\rho < 1 + \sqrt{\nu}/E$.

Generally speaking, N_c^H increases with astigmatism. For example, let us consider the optics case with $0 < \rho < 1 + \sqrt{\nu}/E$ with an input beam (22) that is “focused” along the x direction, i.e., has $E > 1$. As E increases it will approach the value $E_c = \sqrt{\nu}/(\rho - 1)$, for which $N_c^H = \infty$. Physically speaking, this results suggests that as the input beam becomes narrower along the x axis, the critical power for collapse increases, making the collapse more difficult to attain. This conclusion is also consistent with the numerical observations of Crasovan et al. [13] in the optics case, and is in the same spirit as the results of Fibich and Ilan [31] for the NLS case (i.e., $\rho = 0$).

Similar to the symmetric case, for a given power N , the separatrix curve in the (ν, ρ) plane for which $H = 0$ is given by

$$\rho_c^H(N, \nu, E) \equiv \left[1 - \frac{(E + 1/E)\pi}{N} \right] \left(1 + \frac{\sqrt{\nu}}{E} \right), \tag{25}$$

such that when $\rho < \rho_c^H$ then $H < 0$ and, therefore, collapse is guaranteed by the Virial Theorem.

4.2 Another, related NLSM-type system

Suppose we consider the NLSM System (4), but without the cubic term $|u|^2u$, i.e.,

$$iu_z + \frac{1}{2}\Delta u - \rho u\phi_x = 0, \tag{26a}$$

$$\phi_{xx} + \nu\phi_{yy} = (|u|^2)_x. \tag{26b}$$

It is natural to expect that the collapse mechanisms in the above NLSM-type System (26) would be similar to the NLSM System (4). Indeed, the analysis of System (26) is quite similar to that in sections 3 and 4. A difference is that the Hamiltonian corresponding to (26) is like (13), but without the second “self-focusing” integral, that is,

$$H(u, \phi) = \frac{1}{2} \int |\nabla u|^2 + \frac{\rho}{2} \int (\phi_x^2 + \nu\phi_y^2).$$

Since the Virial Theorem (13) remains unchanged, collapse is possible in System (26) whenever $\rho < 0$ and the initial conditions are sufficiently large. If $\rho > 0$ then the system is of defocusing type and no collapse occurs. Furthermore, substituting the initial-conditions (18) into the Hamiltonian above gives

$$H(u_0, \phi_0) = N + \frac{\rho}{1 + \sqrt{\nu}} \frac{N^2}{2\pi}.$$

It follows that the threshold power for which $H = 0$ is given by

$$N_c^H(\nu, \rho) \equiv -\frac{2\pi(1 + \sqrt{\nu})}{\rho}.$$

Thus, similar to the NLSM case, the Virial Theorem guarantees that the solution of System (26) undergoes finite-distance collapse when $N > N_c^H$. Thus, although the cubic term in the NLSM System (4) is self-focusing, its presence is not necessary for collapse to occur. In other words, collapse can occur even in the case when the nonlinearity is strictly and strongly nonlocal.

5 Ground-states and astigmatism

Below we study how the astigmatism of the ground-state depends on ρ and ν . The astigmatism is recovered from the ground-state with the following definition

$$e(F) \equiv \frac{\int |(F^2)_x|}{\int |(F^2)_y|}. \quad (27)$$

It follows from (27) that $e = 1$ corresponds to a radially-symmetric ground-state, and $e < 1$ and $e > 1$ correspond to a ground-state that is relatively wider along the x and y axes, respectively. In other words, $e \approx L_y/L_x$, where L_x and L_y are the full-widths at half-max of the function.

Figure 4(a,b) depicts the “on-axes” amplitudes of the ground-state for $\rho = 0$ (i.e., the radially-symmetric R profile); $(\nu, \rho) = (1, -2)$; and $(\nu, \rho) = (1, 2)$. The contour plots in figure 4(c) and (d) correspond to the $\rho = -2$ and $\rho = 2$ cases, respectively. These plots demonstrate that the ground-states with $\rho \neq 0$ can be astigmatic.

Figure 5 shows contour plots associated with the 3D calculation of the ground-state for $(\nu, \rho) = (3, -5)$, which has $e \approx 1.52$. Both $F(x, y)$ and the corresponding mean field $G(x, y)$ are certainly astigmatic. Furthermore, the mean field G is strongly nonlocal (see also figure 5(d)), as can be expected from the Poisson-type equation (14b) that it is obtained from.

Figure 6(a) shows that (i) the NLS ground-state ($\rho = 0$) is radially-symmetric, (i.e., $e = 1$); (ii) when $\nu = 0.5$ and $\rho < 0$ (water-waves case) F is wider along the y -axis (i.e., $e > 1$); and (iii) when $\nu = 0.5$ and $\rho > 0$ (optics case) F is wider along the x -axis (i.e., $e < 1$). We note that the parameter space explored in figure 1 and figure 6a is the same. Comparing these two figures, one sees that as ρ is changed from $\rho = 0$ (in either direction), the deviation from the NLS ground state is accompanied by a significant deviation in the critical power, as well as by a deviation from radial-symmetry. Therefore, as $|N_c(\nu, \rho) - N_c(\nu, 0)|$ increases with ρ , so does the astigmatism of the ground-state (along the x or y axes). On the other hand, figure 2 and

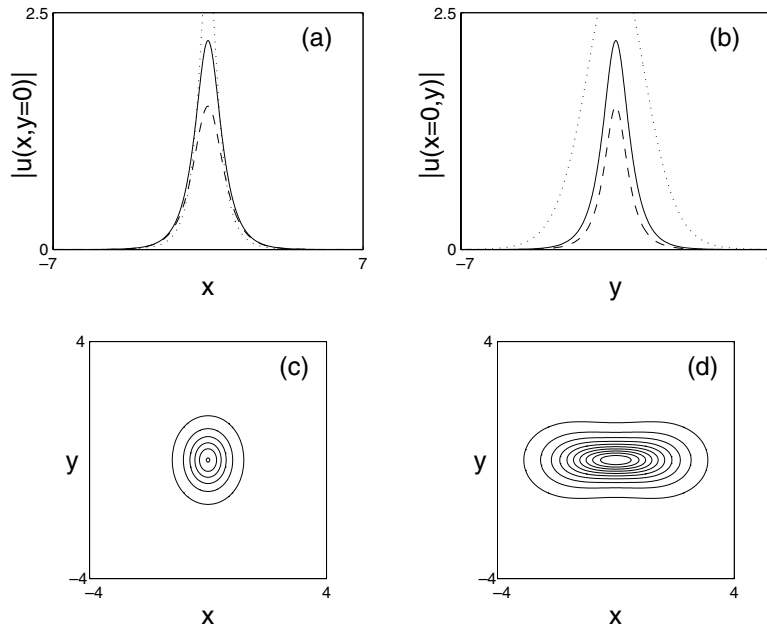


Fig. 4. Top: the on-axes amplitudes of the ground-state (a) along the y -axis and (b) along the x -axis for $(\nu, \rho) = (1, 2)$ (dashes), $\rho = 0$ (solid), and $(\nu, \rho) = (1, -2)$ (dotted). Bottom: contour plots of $F(x, y)$ for: (c) $\rho = -2$ (corresponding to dotted above) with astigmatism [i.e. equation (27)] $e \approx 1.29$; (d) $\rho = 2$ (corresponding to dashes above) with $e \approx 0.33$.

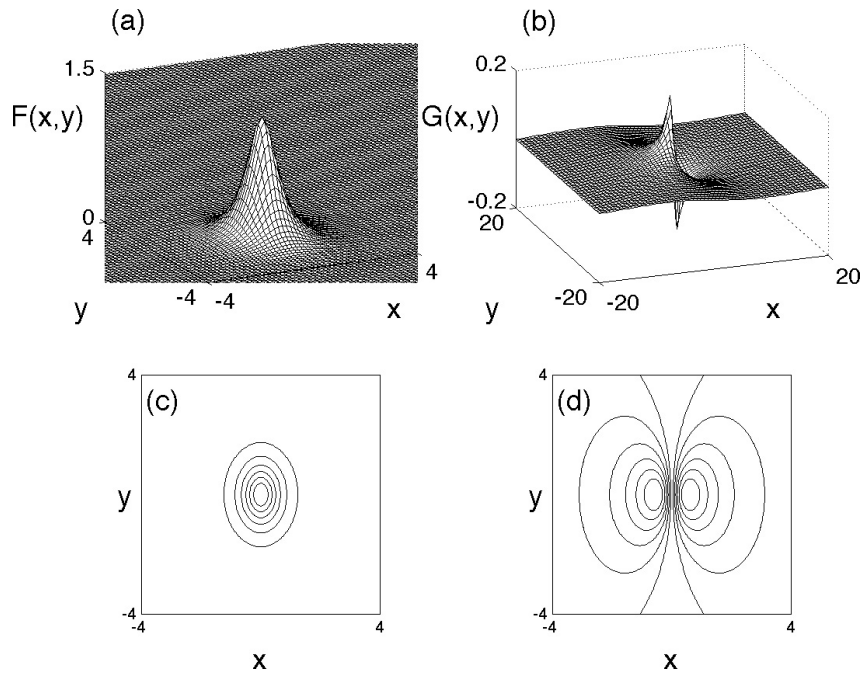


Fig. 5. The ground-state [i.e., solution of System (14)] for $(\nu, \rho) = (3, -5)$. (a) and (b) are 3D plot of $F(x, y)$ (for which $e \approx 1.52$) and $G(x, y)$, respectively; (c) and (d) are contour plots corresponding to (a) and (b), respectively.

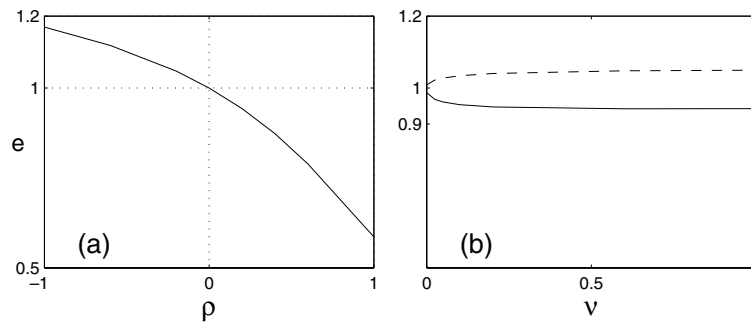


Fig. 6. The astigmatism (27) of the ground-state $F(x, y)$ of System (4) for: (a) $\nu = 0.5$ with $-1 \leq \rho \leq 1$ (i.e., same as figure 1); (b) $\rho = -0.2$ (dashes) and $\rho = 0.2$ (solid) with $0 \leq \nu \leq 1$ (i.e., same as figure 2a and 2b, respectively).

figure 6(b) show that the critical power and the astigmatism are only weakly dependent on ν , for either sign of ρ . In addition, figure 6(a) shows that, for the same values of ν , the function F is relatively more astigmatic for $\rho > 0$ (i.e., for optics) than for $\rho < 0$ (i.e., for water waves).

6 Quasi self-similar collapse is astigmatic

Detailed asymptotic analysis and careful numerical simulations strongly suggest that when collapse occurs in NLS equation (1), under quite general conditions, it occurs with a quasi self-similar profile that is a modulation (up to a phase) of the ground-state (cf. [8]), namely as $z \rightarrow Z_c$, Z_c being the collapse distance (or time),

$$|u(x, y, z)| \sim \frac{1}{L(z)} R\left(\frac{r}{L(z)}\right), \tag{28}$$

where (x, y) are in a region surrounding of the collapse point (which typically shrinks during the self-focusing process), $R(r)$ is the NLS ground-state (see section 3), and $L(z)$ is a modulation function, such that $\lim_{z \rightarrow Z_c} L(z) = 0$. In the NLS case, the ground-state $R(r)$ is radially-symmetric and, so far as we are aware, all NLS-collapse simulations to date have shown that collapse occurs with a radially-symmetric profile. The quasi self-similar collapse has received much theoretical attention since the contribution of Merle and Tsutsumi [32]. But, it is very difficult to justify (28) rigorously. Only recently did Merle and Raphael [9] provide sharp results explaining this quasi self-similar behavior in the case of the NLS equation (1).

In contrast to the NLS case, when $\rho \neq 0$ and $\nu > 0$ the NLSM System (4) is not rotationally invariant and the stationary solutions of (14) are not radially symmetric. Moreover, in this parameter regime the stationary solutions cannot be transformed into radially-symmetric functions by any rescaling of x and y . Therefore, the NLSM ground-state, $F(x, y)$, is inherently astigmatic, which makes the analysis and numerical simulations more difficult. The asymptotic analysis of Papanicolaou et al. [14] indicates that, similar to the NLS collapse, NLSM collapse occurs with a modulated profile, i.e.,

$$|u(x, y, z)| \sim \frac{1}{L(z)} P\left(\frac{x}{L(z)}, \frac{y}{L(z)}, b(z)\right), \quad (29)$$

for certain functions $P(x, y)$, $L(z)$, and $b(z)$, such that as $z \rightarrow Z_c$, $L(z)$ and $b(z)$ approach zero and $P(x, y)$ asymptotically approaches the ground-state function F . Numerical simulations of the NLSM using “dynamic rescaling” suggested that the collapsing solution does approach a modulated profile. The numerical results in this section suggest that up to moderately small values of $L(z)$, the amplitude of the collapsing solution behaves as

$$|u(x, y, z)| \sim \frac{1}{L(z)} F\left(\frac{x}{L(z)}, \frac{y}{L(z)}\right), \quad (30)$$

where $F(x, y)$ is the ground-state of System (4). These results complement those in [14]. Here the NLSM solution is directly compared to the corresponding ground-state itself. Previously researchers did not calculate the ground state.

To study NLSM collapse numerically, System (4) is solved with the Gaussian initial conditions (18). The self-focusing dynamics are recovered from the simulations using the so-called “focusing factor”, $|u(0, 0, z)|/|u_0(0, 0)|$, as a function of the propagation distance z . The astigmatism of the solution is recovered in accordance with (27) as

$$e(z) = \frac{\int |(|u|^2)_x|}{\int |(|u|^2)_y|}. \quad (31)$$

We begin by presenting several numerical simulations of collapse, that also serve to verify some of the results of the previous sections. As noted in section 3, the Hamiltonian of the NLSM suggests that the water-waves case ($\rho < 0$) is “more focusing” than the optics case ($\rho > 0$). Indeed, figure 7 shows that when the same initial conditions are used for all cases, collapse with $\rho = -1$ precedes collapse with $\rho = 0$, which, in turn precedes collapse with $\rho = 1$. For this figure, the input power is taken as $1.2N_c(\nu = 0.5, \rho = 1) \approx 12.2$. We note that this value of N_c is approximately twice as large as $N_c(R)$ and approximately 3.3 times larger than $N_c(\nu = 0.5, \rho = -1)$ (see figure 1).

Since $\rho < 0$ and $\rho > 0$ correspond water waves and optics, respectively, and since critical power depends on ρ , a somewhat more “balanced” comparison between the water-waves and optics cases uses the same initial conditions, but with an input power chosen with respect to the corresponding critical power (which is different for water-waves and optics). Therefore, in the simulations below [i.e., figures 8–13] we use the input power $N = 1.2N_c(\nu, \rho)$, i.e., this is 20% above the corresponding critical power for collapse. Figure 8(a) shows the dynamics of the focusing factor for $\nu = 0.5$ with: $\rho = 0$ (NLS), $\rho = 1$ (optics), and $\rho = -1$ (water waves).

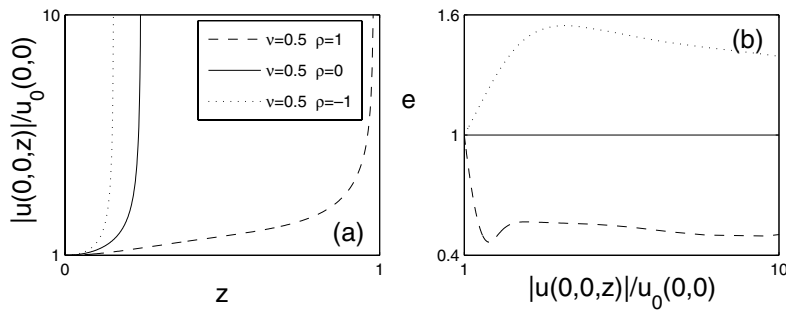


Fig. 7. (a) The focusing factor associated with the NLSM solutions [i.e., System (4)] using $\nu = 0.5$ and three values of ρ (see legend) using the initial conditions (18) with the same input power $N = 1.2N_c(\nu = 0.5, \rho = -1) \approx 12.2$. (b) The corresponding astigmatism (31) of the solution as a function of the focusing factor.

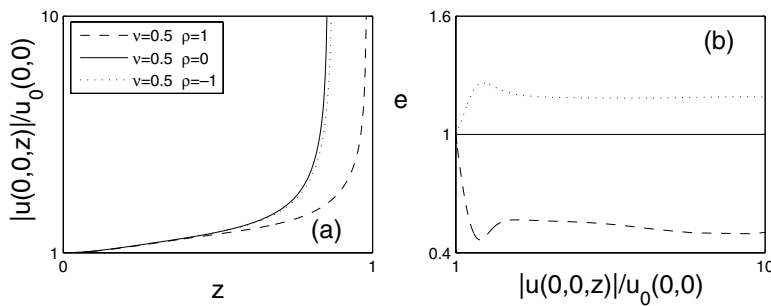


Fig. 8. Same as figure 7, but here using the input power $N = 1.2N_c(\nu, \rho)$, i.e., 20% above the corresponding critical power.

Similarly to figure 7, the collapse distance with $\rho > 0$ is greater than with $\rho \leq 0$. Surprisingly, the collapse distance in the $\rho = 0$ and $\rho < 0$ cases is nearly the same. Although one might have expected the collapse with $\rho < 0$ to precede collapse with $\rho = 0$ (as in figure 7), this is not the case here, because $N(\rho = -1)$ is approximately 1.6 times smaller than $N(\rho = 0)$ (see figure 3). Thus, in figure 8 the collapse distances of the $\rho = -1$ and $\rho = 0$ simulations are close, because the input power in the $\rho = -1$ simulation is much larger than the input power in the $\rho = 0$ case.

In addition, figure 8(b) contains the corresponding astigmatism plots. The astigmatism is plotted as a function of the focusing factor (rather than as a function of z) in order to “blow up” the dynamics near the collapse point, where the interesting changes in the astigmatism are expected to occur. While the NLS solution remains radially-symmetric (i.e., $e \equiv 1$), the NLSM solutions become astigmatic during propagation. Furthermore, $\rho < 0$ and $\rho > 0$ correspond to $e > 1$ and $e < 1$, respectively, which is consistent with in figures 4 and 6. As can be seen from this figure, at the initial stage of the propagation the astigmatism of the NLSM solutions becomes large, in a direction that depends on ρ . Based on these simulations it appears that the astigmatism nearly approaches a constant value in the neighborhood of the collapse point, which is a value that depends on ν and ρ (such that $e \neq 1$). This is consistent with the results in [14], as well as with the results presented below.

Figures 7–9 indicate that NLSM collapse is astigmatic, but they do not show that the collapse process is quasi self-similar. In order to study the self-similarity of the collapse process, in accordance with equation (30), the modulation function is recovered from the solution as

$$L(z) = \frac{F(0, 0)}{|u(0, 0, z)|},$$

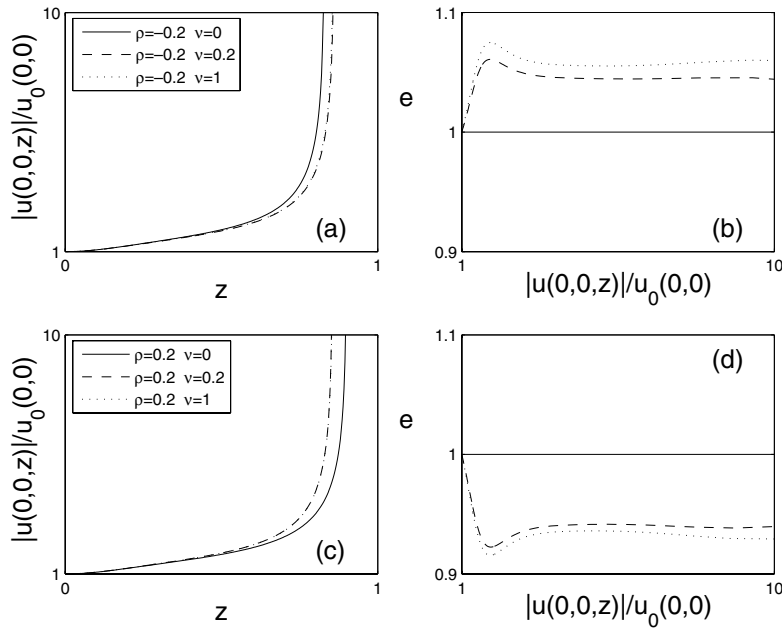


Fig. 9. Same as figure 8 with [(a),(b)] $\rho = -0.2$ and $\nu = 0$ (solid), $\nu = 0.2$ (dashes), and $\nu = 1$ (dotted, on top of the dashes); [(c),(d)] same as above with $\rho = 0.2$.

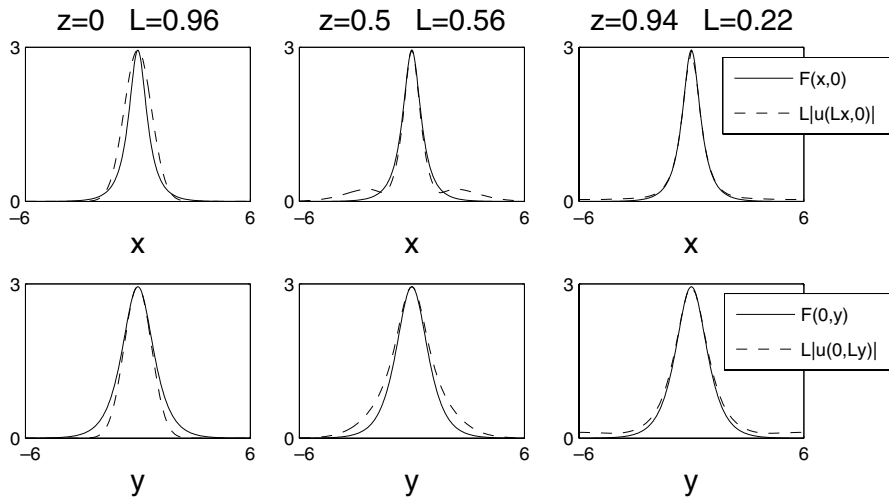


Fig. 10. Convergence of the wave collapse profile (dashes) to the NLSM ground state (solid) along the x axis (top) and the y axis (bottom) with $(\nu, \rho) = (0.5, 1)$. The initial conditions are (18) with $N = 1.2N_c(\nu, \rho)$.

where $F(x, y)$ is the corresponding ground-state. The rescaled amplitude of the solution of the NLSM, $L(z)|u(L(z)\tilde{x}, L(z)\tilde{y}, z)|$, is then compared with $F(\tilde{x}, \tilde{y})$, where $F(\tilde{x}, \tilde{y})$ is the ground-state and $(\tilde{x}, \tilde{y}) = (L(z)x, L(z)y)$. If indeed the collapse process is quasi self-similar with the corresponding ground-state, the rescaled amplitude should converge pointwise to F in a neighborhood of the origin as $z \rightarrow Z_c$ (i.e., near the collapse point).

Figure 10 shows that the NLSM collapse is indeed self-similar with the ground-state for $\nu = 0.5$ and $\rho = 1$. The rescaled on-axis amplitude is compared separately on the x and y axes (top and bottom plots, respectively). One can see that, as the solution is undergoing

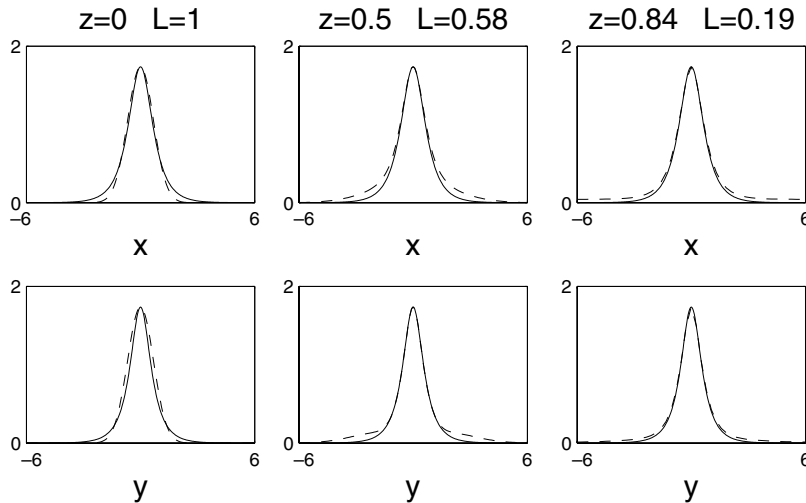


Fig. 11. Same as figure 10 with $(\nu, \rho) = (0.5, -1)$.

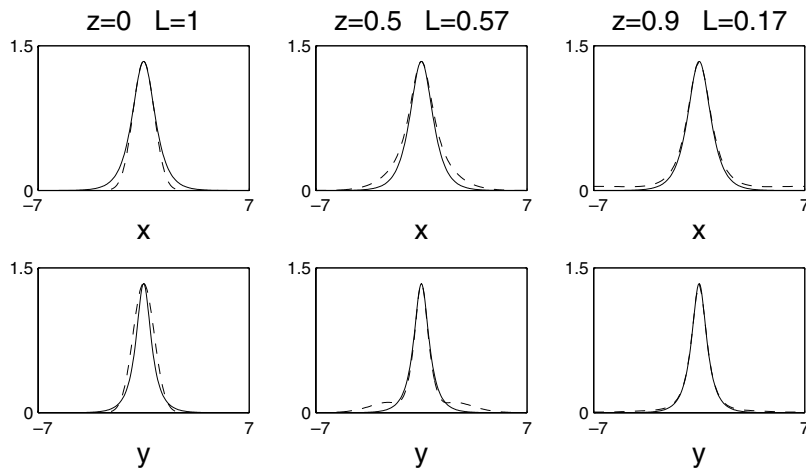


Fig. 12. Same as figure 10 with $(\nu, \rho) = (4, -4)$.

self-focusing [i.e, as $L(z)$ approached zero], its rescaled profile approaches that of the astigmatic ground-state near the origin.

Figure 11 shows the same situation, but with $\rho = -1$, whose ground-state is somewhat less astigmatic than with $\rho = 1$. In order to observe self-similar collapse with $\rho < 0$ and a more astigmatic profile, figure 12 compares the solution and the ground-state with $\nu = 4$ and $\rho = -4$. The ground-state in this latter case is clearly more astigmatic. Nevertheless the collapse process is quasi self-similar with the ground-state. figure 13 further demonstrates the local nature of the self-similar collapse process. While the spatial region in the vicinity of the collapse point is self-similar to the ground-state, the outer “wings” of the solution do not approach the ground-state. This phenomenon is also well-known in the NLS case as well [8], and can be understood as follows: in accordance with equation (30), only one critical power enters the collapse region. More precisely, as $z \rightarrow Z_c$, the power of $u(x, y, z)$ contained in a “ball” of radius $L(z)$ around the collapse point is just slightly above N_c (cf. [32]). Since the input power is 20% above N_c , the residual 20% is radiated into the outer wings in a process that is not quasi self-similar with the ground-state.

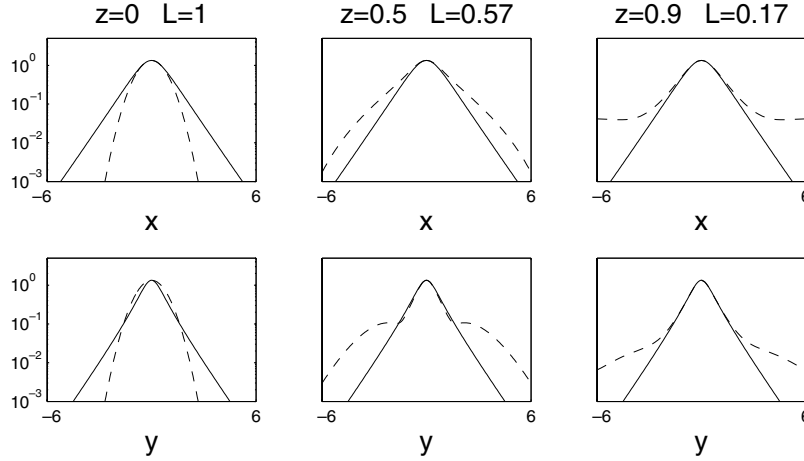


Fig. 13. Same as figure 12 on a semi-log plot.

7 Arrest of wave collapse

Collapse with an infinite amplitude does not actually occur in physical situations. In reality, there are always physical mechanisms that arrest the collapse. Such mechanisms have been studied extensively in nonlinear optics, e.g., nonlinear saturation [33,34], beam nonparaxiality [35], and vectorial effects [36]. In order to investigate such arrest of collapse in NLSM, we briefly investigate the NLSM with a small nonlinear saturation of the cubic nonlinearity given by

$$iu_z + \frac{1}{2}\Delta u + \frac{|u|^2 u}{1 + \varepsilon|u|^2} - \rho u \phi_x = 0, \quad (32a)$$

$$\phi_{xx} + \nu \phi_{yy} = (|u|^2)_x, \quad (32b)$$

where ε is the small nonlinear-saturation parameter.

When $\rho \ll 1$ and $\varepsilon \ll 1$ System (32) is a small perturbation of the NLS equation (1). In that case, the asymptotic analysis of Fibich and Papanicolaou [15] for the perturbed NLS can be used. Their analysis is based on the asymptotic and numerical observations that the collapsing solution in the NLS case is quasi self-similar with the ground-state (Townes profile), i.e., as in equation (28). Asymptotic analysis shows that, to leading order, the dynamics of the focusing factor in the solution of System (32) is given by the following ODE (see [5.3–5.4], [15])

$$(w_z)^2 = -\frac{4H_0}{M} \frac{(w_M - w)(w - w_m)}{w}, \quad (33)$$

where $w(z) = L^2(z)$, $L(z)$ is the focusing-factor in equation (28), $M \approx 0.55$, and H_0 , w_M , and w_m are constants that depend only on ε and the initial conditions, such that $w_M > w_m$. It follows from this nonlinear-oscillator-type equation that for generic initial conditions the intensity of the solution initially focuses [i.e., $L(z)$ decreases] until $L \sim \sqrt{w_m} = O(\sqrt{\varepsilon})$, then defocuses [i.e., $L(z)$ increases] until $L \sim \sqrt{w_M}$, followed by focusing-defocusing oscillations, such that $\sqrt{w_m} \leq L(z) \leq \sqrt{w_M}$.

Figure 14 shows the on-axis amplitude of the numerical solution of System (32) for $\rho = -4$, $\nu = 4$, $\varepsilon = 0.0025$, and the initial conditions (18) with $N = 1.2N_c$, where N_c is the critical power corresponding to $\varepsilon = 0$. We note that ρ is quite large and, therefore, System (32) is *not* a small perturbation of the NLS equation (1). Surprisingly, the numerical solution of System (32) agrees qualitatively with the predictions based on equation (33). Indeed, one sees that collapse is arrested by the small nonlinear saturation, followed by a series of focusing-defocusing oscillations. To understand the success of the asymptotic analysis beyond its formal region of validity, we note that in the absence of the nonlinear saturation in System (32), i.e.,

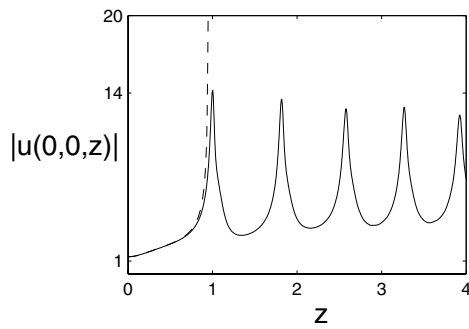


Fig. 14. Collapse in the NLSM system [i.e., System (4) with $(\nu, \rho) = (4, -4)$, dashes] is found to be arrested by small nonlinear saturation [i.e., System (32) with $(\nu, \rho) = (4, -4)$ and $\varepsilon = 0.0025$, solid].

for the NLSM case, the collapse dynamics (e.g., the rate of blowup) is nearly the same as for the NLS case even when ρ is large [14, 15]. Therefore, the additional small nonlinear saturation considered in System (32) has the same effect as though it were a small perturbation of the NLS itself, for which the asymptotic analysis should be valid.

8 Summary and final remarks

Nonlinear-wave systems which have quadratic-cubic type interactions, such as in nonlinear optics and in nonlinear free-surface water waves, lead to the NLSM System (4). The NLSM system is found to admit finite-distance collapse in a certain parameter regime. The regions of collapse and global-existence is explored in a broad range of parameter space and the consistency between global existence theory, the Virial Theorem, and numerical simulations the NLSM System (4) is demonstrated. Importantly, numerical simulations of the NLSM show that the collapse process occurs with a quasi self-similar profile, which is a modulation of the ground-state profile. The ground-state profile is found using a numerical algorithm that was recently used in dispersion-managed NLS theory (cf. [29, 30]). In general, the ground-state profile is astigmatic and, therefore, the collapse profile is astigmatic as well.

These results are in the same spirit as for the NLS equation (1). However, NLSM theory is more complex and not yet as advanced as NLS theory. There are some open questions and problems. For example, as indicated above, it remains to extend the sharp theoretical results on the self-similar nature of the singularity to the NLSM case. From the numerical perspective, while our simulations indicate that NLSM collapse occurs with a self-similar ground-state, we only resolve moderate the simulations to moderately sized focusing factors [i.e., $O(10)$] near the collapse point. Using more specialized numerical methods (cf. [14, 37]), much larger focusing factors (e.g. greater than 10^4) could furnish more convincing evidence of this self-similar collapse. From the experimental perspective, self-similar collapse in quadratic-cubic type media remains to be demonstrated in either free-surface water waves or nonlinear optics.

This research was partially supported by the U.S. Air Force Office of Scientific Research, under grant FA4955-06-1-0237 and by the National Science Foundation, under grants DMS-0303756, DMS-0602151.

References

1. M.J. Lighthill, *Waves in Fluids* (Cambridge Univ. Press, Cambridge, 1978)
2. M.J. Ablowitz, H. Segur, *Solitons and the Inverse Scattering Transform* (SIAM, Philadelphia, 1981)
3. G.B. Whitham, *Linear and Nonlinear Waves* (Wiley, New York, 1974)
4. P.L. Kelley, Phys. Rev. Lett. **15**, 1005 (1965)
5. S. Vlasov, V. Petrishchev, V. Talanov, Radiophys. Quant. Elec. **14**, 1062 (1971)
6. M.I. Weinstein, Commun. Math. Phys. **87**, 567 (1983)

7. G.C. Papanicolaou, D. McLaughlin, M. Weinstein, *Num. Appl. Anal.* **5**, 253 (1982)
8. C. Sulem, P.L. Sulem, *The Nonlinear Schrödinger Equation* (Springer-Verlag, New York, 1999)
9. F. Merle, P. Raphael, *Invent. Math.* **156**, 565 (2004)
10. K.D. Moll, A.L. Gaeta, G. Fibich, *Phys. Rev. Lett.* **90**, 203902 (2003)
11. D.J. Benney, G.J. Roskes, *Stud. Appl. Math.* **48**, 377 (1969)
12. A. Davey, K. Stewartson, *Proc. Roy. Soc. A London* **338**, 101 (1974)
13. L.-C. Crasovan, J.P. Torres, D. Mihalache, L. Torner, *Phys. Rev. Lett.* **91**, 063904 (2003)
14. G.C. Papanicolaou, C. Sulem, P.L. Sulem, X.P. Wang, *Physica D* **72**, 61 (1994)
15. G. Fibich, G.C. Papanicolaou, *SIAM J. Appl. Math.* **60**, 183 (1999)
16. M.J. Ablowitz, H. Segur, *J. Fluid Mech.* **92**, 691 (1979)
17. M.J. Ablowitz, R. Haberman, *Phys. Rev. Lett.* **35**, 1185 (1975)
18. V.D. Djordevic, L.G. Reddekopp, *J. Fluid Mech.* **79**, 703 (1977)
19. A.S. Fokas, M.J. Ablowitz, *Phys. Rev. Lett.* **51**, 7 (1983)
20. M.J. Ablowitz, P.A. Clarkson, *Solitons Nonlinear Evolution Equations and Inverse Scattering* (Cambridge University Press, Cambridge, 1991)
21. R.Y. Chiao, E. Garmire, C.H. Townes, *Phys. Rev. Lett.* **13**, 479 (1964)
22. V.I. Talanov, *Sov. Phys. JETP Lett.* **2**, 138 (1965)
23. M.J. Ablowitz, G. Biondini, S. Blair, *Phys. Lett. A* **236**, 520 (1997)
24. M.J. Ablowitz, G. Biondini, S. Blair, *Phys. Rev. E* **63**, 605 (2001)
25. J.P. Torres, L. Torner, I. Biaggio, M. Segev, *Opt. Comm.* **213**, 351 (2002)
26. J.M. Ghidaglia, J.C. Saut, *Nonlinearity* **3**, 475 (1990)
27. R. Cipolatti, *Comm. Part. Diff. Eq.* **17**, 967 (1992)
28. G. Fibich, A.L. Gaeta, *Opt. Lett.* **25**, 335 (2000)
29. M.J. Ablowitz, Z. Musslimani, *Phys. Rev. E* **67**, 025601(R) (2003)
30. V.I. Petviashvili, *Sov. J. Plasma Phys.* **2**, 257 (1976)
31. G. Fibich, B. Ilan, *J. Opt. Soc. Am. B* **17**, 1749 (2000)
32. F. Merle, Y. Tsutsumi, *J. Diff. Eq.* **84**, 205 (1990)
33. B.I. Cohen, B.F. Lasinski, A.B. Langdon, J.C. Cummings, *Phys. Fluids* **3**, 766 (1992)
34. F. Vidal, T.W. Johnston, *Phys. Rev. Lett.* **77**, 1282 (1996)
35. G. Fibich, *Phys. Rev. Lett.* **76**, 4356 (1996)
36. G. Fibich, B. Ilan, *Physica D* **157**, 113 (2001)
37. G. Fibich, W. Ren, X.P. Wang, *Phys. Rev. E* **67**, 056603 (2003)